ELSEVIER

Journal of Chromatography A, 707 (1995) 217–224

JOURNAL OF CHROMATOGRAPHY A

Normal-phase high-performance liquid chromatography using enhanced-fluidity liquid mobile phases

Stephen T. Lee, Susan V. Olesik*

Department of Chemistry, The Ohio State University, 120 West 18th Avenue, Columbus, OH 43210-1173, USA

First received 22 July 1994; revised manuscript received 8 February 1995; accepted 21 February 1995

Abstract

The application of an enhanced-fluidity liquid mixture (*n*-hexane–CO_2) as a mobile phase in normal-phase HPLC using a 3-cyanopropyl polysiloxane stationary phase was evaluated. Decreased pressure drop across the chromatographic column was observed with increasing proportions of added CO_2 to the mixtures. For selected mixture conditions, increased efficiency and decreased peak asymmetry were obtained in comparison to that for separations with 100% *n*-hexane. A limiting amount of CO_2 that could be added to hexane was found. If more CO_2 was added past that limit, serious peak asymmetry lowered the measured column efficiency.

1. Introduction

High-performance liquid chromatography (HPLC) is presently the most widely used separation technique for nonvolatile compounds. However, HPLC is not without limitations. HPLC typically has larger pressure drops across the chromatographic column, longer analysis times, and lower efficiencies than supercritical fluid chromatography (SFC) or gas chromatography (GC). These deficiencies can be attributed to higher viscosities and lower solute diffusion rates in liquids compared to supercritical fluids or gases. GC and SFC also have limitations: GC is limited to the separation of volatile compounds, while SFC is limited in its ability to chromatograph polar molecules.

Enhanced-fluidity liquid mobile phases provide HPLC some of the advantages of SFC. Enhanced-fluidity mobile phases are prepared by dissolving large proportions of low-viscosity liquids, such as CO_2, in commonly used solvents. It was previously demonstrated in our laboratory that the use of enhanced-fluidity liquids provided mobile phases with low viscosities. In addition, chromatographic advantages such as increased diffusion, lower pressure drops, and decreased analysis times without loss of solvent strength were demonstrated for reversed-phase HPLC [1–3] and for HPLC using a glassy carbon stationary phase [4].

In this paper, we report initial studies of enhanced-fluidity mobile phases in normal-phase HPLC with a hexane–CO_2 mobile phase. Mobile phases in normal-phase chromatography are typically mixtures of a nonpolar solvent, such as hexane, and one or more polar solvents. The polar solvents are added to control the selectivity of the separation. The addition of CO_2 to normal-phase mobile phases should be viewed as

* Corresponding author.

0021-9673/95/$09.50
SSDI 0021-9673(95)00250-2

a fluidity modifier. Especially for the separation of polar solutes, the addition of CO_2 will not affect markedly the selectivity of the separation. As a benchmark characterization, we have concentrated on an evaluation of the hexane–CO_2 mixture with the full understanding that more polar modifiers must be added to this mixture for the separation of polar solutes. An attractive feature of the use of liquid carbon dioxide as a co-solvent in normal-phase HPLC is that when carbon dioxide is included in mixtures, it functions as a homogenizing agent and often allows complete miscibility of solvent pairs with substantially different polarity. [5]

2. Experimental

2.1. Instrumentation

The chromatographic system was previously described [2]. Briefly, it consists of an ISCO LC-2600 syringe pump (ISCO, Lincoln, NE, USA), a Valco W-series high-pressure injection valve with an injection volume of 60 nl (Valco Instruments, Houston, TX, USA), a Deltabond Cyano (3-cyanopropyl polysiloxane stationary phase), 250 × 1 mm I.D. column packed with 5-μm diameter particles containing 300 Å pores with stationary-phase loading of ca. 4% carbon (Keystone Scientific, Bellefonte, PA, USA) and a Spectra-Physics UV2000 UV–Vis absorbance detector equipped with a capillary flow cell mounting (Model 9550-0155). A piece of 50 μm I.D. fused-silica tubing (Polymicro Technologies, Phoenix, AZ, USA) was connected to the end of the column with a zero dead volume fitting; a flow cell was created by removing the polyamide coating from a 5-mm length of the tubing and centering it in the capillary flow cell mounting. The detector excitation wavelength was 210 nm. A Setra 204 series pressure transducer (Setra Systems, Acton, MA, USA) was placed in-line after the detector and before the post-detection restrictor. The outlet pressure was monitored because the column pressure must be maintained above a minimum pressure to prevent the hexane–CO_2 mobile-phase mixture from separating into two phases (liquid/gas). For example, at 25°C and a CO_2 mole fraction of 0.6, the hexane–CO_2 separates into two phases at pressures lower than 4.36 MPa [6]. All experiments in this study were performed under conditions in which the hexane–CO_2 mixture was in a single liquid phase. The flow control for the chromatographic system was maintained by an appropriate length of 8, 15, or 20 μm I.D. fused-silica tubing. The column inlet pressure was maintained at 13.8 MPa throughout this study except when hexane was the mobile phase. When *n*-hexane was used as the mobile-phase higher pressures were necessary to obtain linear velocities above 0.22 cm/s. Data were collected on a strip chart recorder (Linear Instruments, Reno, NV, USA).

Column efficiency, N, was calculated manually via the method developed by Foley and Dorsey [7] (Eq. 1):

$$N = \frac{41.7(t_r/W_{0.1})^2}{B/A + 1.25} \quad (1)$$

where t_r is retention time, $W_{0.1}$ is the width of the chromatographic band at 10% of the peak's height and B/A is a an empirical asymmetry factor. A and B are referenced to the peak maximum with $A + B = W_{0.1}$ [8]. This calculation is based on the exponentially modified Gaussian model (Eq. 2):

$$N = \frac{t_r^2}{\sigma_G^2 + \tau^2} \quad (2)$$

where σ is the standard deviation of the Gaussian function and τ is the time constant of the exponential. Two independent studies recently showed that Foley and Dorsey's method is the most accurate means to manually determine chromatographic column efficiency [9,10].

The solvent strength was characterized by measuring the Kamlet–Taft π^* parameter for the hexane–CO_2 mixtures. To determine the π^* parameter the solvatochromic shift of the ortho-nitroanisole UV–Vis spectrum was measured [11]. A DMS-100 UV–Vis (Varian, Sunnyvale, CA, USA) was used in these studies. The π^* parameter was calculated using Eq. 5 [11]:

$$\pi^* = \frac{\nu_{max} - \nu_0}{s} \quad (3)$$

where ν_{max} is the frequency of the absorbance maximum of *o*-nitroanisole, when dissolved in the solvent of interest, ν_0 is the frequency of the absorbance maximum for the molecular probe in a reference solvent (typically cyclohexane), and s is a proportionality constant that limits the values of π^* to a range of 0 to 1 for common solvents. The literature value of s for *o*-nitroanisole, -2.428 ± 0.195 kK, was used to calculate π^* in these experiments [12]. Cyclohexane was used as the reference solvent. The absorption spectrum was obtained using a home-made, stainless-steel, high-pressure, optical flow cell with an internal volume of 10 ml and an optical path-length of 3.5 cm. The optical path was terminated on each end with cylindrical quartz windows that were 2.86 cm diam. by 1.75 cm thick (ESCO Prod., Oak Ridge, NJ, USA). The optical cell was sealed with Teflon O-rings. The concentration of *o*-nitroanisole used in these studies was approximately $1 \cdot 10^{-4}$ *M*.

2.2. Materials

The test analytes used in this study were phenetole, methyl benzoate, nitrobenzene, and dimethyl phthalate. The concentrations of the analytes were 4830 ppm phenetole, 5470 ppm methyl benzoate, 5950 ppm dimethyl phthalate, and 3590 ppm nitrobenzene in pentane. Pentane was unretained. Supercritical fluid grade CO_2 from Scott Specialty Gases (Plumsteadville, PA, USA) and 99 + % hexane from Aldrich Chemical (Milwaukee, WI, USA) were used as purchased. Hexane–CO_2 mixtures were prepared using two high-pressure syringe pumps. A known volume of hexane was placed in one pump. Liquid CO_2 at 13.8 MPa and 25°C was held in another pump. Using the known density of CO_2 at these conditions the appropriate volume of CO_2 was calculated and then delivered to the pump holding the hexane to make a given hexane–CO_2 mixture. The mixture was then pressurized to 13.8 MPa and allowed to equilibrate at 25°C for at least 12 h to ensure complete mixing of the solution. This waiting period was not necessary for these mixtures because they are highly miscible. However this is standard procedure for all mixtures that we make in a syringe pump by this means. The completeness of mixing was then checked by monitoring the reproducibility of the solute capacity factors for a given composition.

3. Results and discussion

3.1. Viscosity and pressure drop

The viscosity of the mobile-phase mixtures (Fig. 1) was estimated using the estimation methods of Teja and Rice, and Grunberg and Nissan [13]. The mixture viscosity decreases substantially with increasing proportions of CO_2. As expected when the viscosity of the mobile phase decreases, the pressure drop across the column also decreases for the same linear velocity. Table 1 shows the pressure drop measured across the system for comparable linear velocities with different mobile-phase compositions. The pressure drop across the column decreased by a factor of approximately 6.5 when the mobile-phase mixture was varied from 100% *n*-hexane to 100% CO_2.

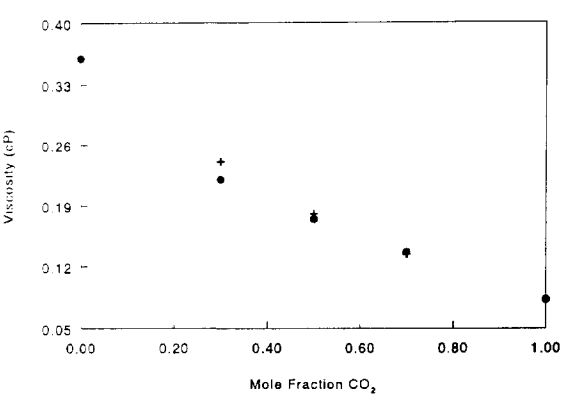

Fig. 1. Estimated viscosity of mobile phases at 25°C and 13.8 MPa: the Grunberg and Nissan method [13] (+); the Teja and Rice method [13] (●).

Table 1
Variation in pressure drop across the chromatographic column with mobile-phase conditions

Mole fraction CO_2	Linear velocity (cm/s)	Pressure drop (MPa)
0.0	0.121	6.18
0.33	0.118	5.40
0.5	0.121	4.18
0.7	0.121	1.53
1.0	0.116	0.95

3.2. Diffusion coefficients

Various empirical expressions have been used to describe the relationship between the viscosity of a solvent and solute diffusivity. Eq. 1 has proven to be the most accurate relationship for predicting diffusion coefficients from solvent viscosities for nonaqueous and mixed solvents over a wide range of temperatures and viscosities [13,14].

$$D_m = A\eta^p \quad (4)$$

where D_m is the diffusion coefficient of a given solute, η is the viscosity of the solvent and A and p are parameters that are characteristic of the solute. A and p can be readily determined from the radius of the solute [15]. Using Bondi radii [16] for the studied solutes, the p parameter is approximately 0.9. Therefore from Eq. 1, the diffusion coefficients for the studied solutes are expected to vary approximately inversely with the viscosity of the mobile-phase mixture (Fig. 1).

3.3. Retention

Fig. 2 shows the variation in capacity factor with mobile-phase composition. The capacity factors of nitrobenzene and dimethyl phthalate decreased with increasing proportions of liquid carbon dioxide added to the mobile phase. Minimum capacity factor values were reached at a CO_2 mole fraction of 0.70. Also as the mole fraction of CO_2 is increased the selectivity of the separation decreases. Fig. 3A is a chromatogram

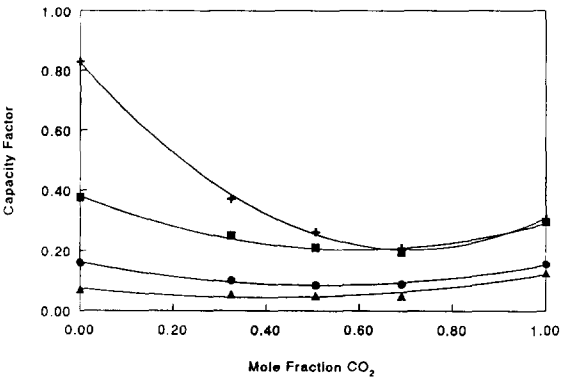

Fig. 2. Variation in capacity factor with mobile-phase composition: phenetole (▲); methyl benzoate (●); nitrobenzene (■); dimethyl phthalate (+). 95% confidence intervals are within the size of the marker. Lines are added as a guide to the eye.

of the test solutes with n-hexane as the mobile phase, while Fig. 3B is a chromatogram of the test solutes with 0.50:0.50 mole fraction of n-hexane–CO_2 as the mobile phase at the same linear velocity. This comparison illustrates the reduction in retention and selectivity with a 0.50:0.50 mole fraction of n-hexane–CO_2 mobile phase.

From the data in Figs. 2 and 3, the addition of CO_2 to hexane clearly increases the mobile-phase solvent strength. Retention of solutes is expected to decrease as the polarity of the solvent increases. The Kamlet–Taft π^* parameter was measured for the hexane–CO_2 mixtures. π^* is a measure of solvent polarizability and dipolarity. Fig. 4 shows that as more CO_2 is added to the mixture, the π^* of the mixture also increases. Interestingly, the π^* parameter of the mixture begins to reach an asymptote near a CO_2 mole fraction of 0.70 which is where the capacity factor levels off as well. Electron donor–acceptor complexing of CO_2 with unsaturated compounds, such as alkenes and benzene [17,18] is well documented. Therefore another possible reason for the diminished retention with the addition of CO_2 is that similar complexation with the cyano-functionality of the stationary phase might occur. More studies are required to understand better the exact reason for the retention variation.

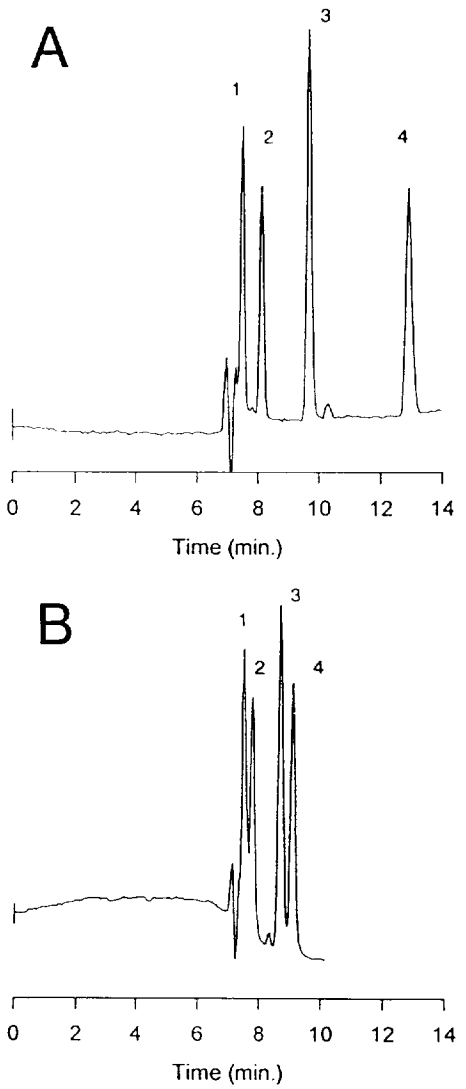

Fig. 3. Chromatograms at 13.8 MPa and 25°C: (A) with *n*-hexane as the mobile phase, and (B) with 0.50 mole fraction of CO_2 in hexane as the mobile phase. Peaks: 1 = phenetole, 2 = methyl benzoate, 3 = nitrobenzene, and 4 = dimethyl phthalate.

3.4. Band dispersion and efficiency

The non-coupled Van Deemter equation shows the relationship between the column band dispersion or plate height, H, and linear velocity of the mobile phase, u:

$$H = A + \frac{B}{u} + Cu \tag{5}$$

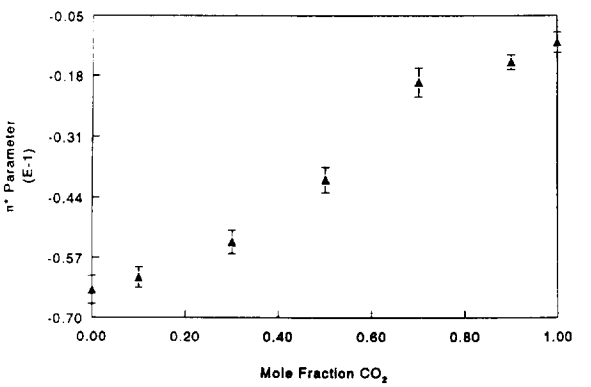

Fig. 4. Variation in the Kamlet–Taft π^* parameter as a function of mobile-phase composition. Error bars indicate 95% confidence intervals.

where A and B are measures of the band dispersion from multiple flow paths and longitudinal diffusion, respectively, and C is a measure of the summation of band dispersion caused by the combined resistance to mass transfer in the mobile phase, the stagnant mobile phase that is present in the pores of the particles, and the stationary phase. In packed columns, $B = \gamma D_m$, where γ is an obstruction factor and D_m is the diffusion coefficient of the solute in the mobile phase. The resistance to mass transfer in the mobile and stagnant mobile phases in the particle pores can be expressed as $C_{m,sm} = f(k')/D_m$, where k' is the capacity factor.

In most HPLC separations, the linear velocity used is such that the C terms are the major cause of band dispersion in the column. Also, when microporous particles are used, the C_{sm} term (due to dispersion in the stagnant mobile phase in the pores) often predominates [19]. If the packing particles are spherical, the following expression describes the variables that control the C_{sm} term:

$$C_{sm} = \frac{(1 - \phi + k')^2 d_p^2 u}{30(1 - \phi)(1 + k')^2 \gamma D_m} \tag{6}$$

where ϕ is the fraction of total mobile phase in the intraparticle space, and γ is the tortuosity factor. Since the diffusion coefficient of the solute is inversely related to solvent viscosity,

from Eq. 6, the C_{sm} term is expected to decrease with decreasing mobile-phase viscosity. Over the limited range of viscosities possible with common liquid mobile phases in normal-phase liquid chromatography using bonded phases, this is clearly the experimentally observed trend [20]. Therefore if diffusion in the stagnant mobile phase controls band dispersion in the present system, then from Eq. 6, the addition of CO_2 to hexane should cause decreased band dispersion due to increased solute diffusion coefficients as long as the capacity factors do not increase with the addition of CO_2.

Also when the first derivative of the van Deemter equation is taken with respect to u, set equal to zero, and the definitions of B and C are substituted, we obtain the following expression:

$$u_{opt} \propto \frac{D_m}{\sqrt{f(k')}} \tag{7}$$

This relationship predicts that if diffusion is the rate-limiting step in the mass transfer process, then as the diffusion coefficient of a solute increases, a corresponding shift in the optimum linear velocity should occur when all other factors remain the same.

To evaluate the effect of mobile-phase composition on band dispersion, the variation of plate height with linear velocity was determined for nitrobenzene and dimethyl phthalate for mobile-phase compositions of 0.0, 0.33, 0.50, 0.70, and 1.0 mole fractions of CO_2 in *n*-hexane at 26°C and 13.8 MPa. Eq. 1 was used to calculate the plate heights from the experimental peak shapes.

Figs. 5A and 5B show the reduced plate height versus linear velocity (0.00–0.40 cm/s) for nitrobenzene and dimethyl phthalate, respectively. For both analytes, there is no observable shift in the optimum velocity as a function of added CO_2 to the mobile phase. For high linear velocities, the slope of the reduced plate height versus linear velocity plots for dimethyl phthalate decreased when CO_2 was added to hexane for the following mixtures: 0.00 mole fraction of CO_2, 0.33 mole fraction of CO_2, 0.50 mole fraction of CO_2. For nitrobenzene, the slopes of these curves for the same mobile-phase compositions

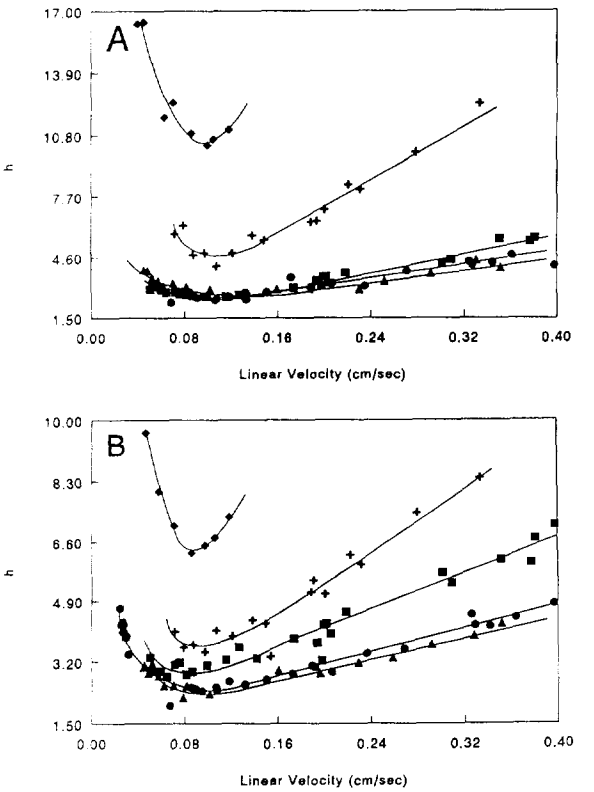

Fig. 5. Variation of reduced plate height of (A) nitrobenzene and (B) dimethyl phthalate as a function of mobile-phase linear velocity at 13.8 MPa for different mobile-phase compositions: *n*-hexane (■); 0.33 mole fraction of CO_2 in hexane (●); 0.50 mole fraction of CO_2 in hexane (▲); 0.70 mole fraction of CO_2 in hexane (+); CO_2 (◆). Average relative standard deviation of the data was 5%.

were statistically the same. By comparing Fig. 5A and Fig. 5B and knowing that the capacity factor of dimethyl phthalate decreased significantly with increased CO_2 while that of nitrobenzene decreased minimally (see Fig. 2), it is clear that the decrease in plate height with added CO_2 for dimethyl phthalate was primarily due to the capacity factor change, and not to a decrease in diffusion coefficient. Also interestingly, instead of seeing a further enhancement in efficiency when the added CO_2 was greater than the 0.50 mole fraction, the reduced plate height dramatically increases for mobile-phase compositions of 0.70 and 1.00 mole fractions of CO_2 in *n*-hexane.

Fig. 6 shows the variation in asymmetry factor,

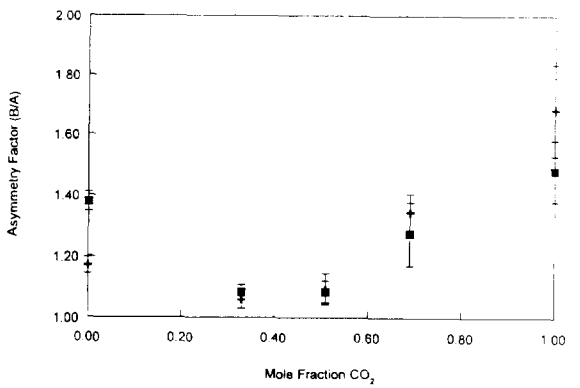

Fig. 6. Variation in peak asymmetry (B/A) with mobile-phase composition: nitrobenzene (+); dimethyl phthalate (■). Error bars indicate 95% confidence intervals.

B/A, with mobile-phase composition over the linear velocity range 0.00–0.12 cm/s. The observed trend in the plate height measurements correlates closely with the variation in the peak asymmetry factor over the same mobile-phase compositions. Peak tailing is lowest for nitrobenzene and dimethyl phthalate with mobile-phase compositions of 0.33 and 0.50 mole fractions of CO_2 in *n*-hexane and increases markedly for 0.70 and 1.00 mole fractions of CO_2 in neat *n*-hexane. The asymmetry factor was also measured for the two solutes over the 0.16–0.24 cm/s linear velocity range. The shape of the curve of B/A versus CO_2 mole fraction was the same as that observed in Fig. 6 for the lower flow-rate conditions. The major difference between the measured asymmetry factors for the two linear velocities ranges is that the magnitude of the asymmetry factor is greater for the higher linear velocity conditions. For example, the asymmetry factor for 0.70 mole fraction of CO_2 in *n*-hexane at the higher linear velocities was 1.82 and 1.67 for nitrobenzene and dimethyl phthalate, respectively, which is substantially higher than the B/A values observed at the lower linear velocities. The asymmetry factor for the 0, 0.33, and 0.50 mole fractions of CO_2 in *n*-hexane mobile-phase compositions did not vary substantially with linear velocity. The measured peak asymmetry did not vary with solute concentration. From a comparison of the band dispersion data in Fig. 5 with the peak asymmetry data in Fig. 6 and a careful look at the data used to calculate plate heights, it is clear that the peak asymmetry caused the variation in the measured plate height.

Many possible causes for the observed variations in plate height and peak asymmetry exist [21]. The surfaces of chemically bonded stationary phases are often heterogeneous. For moderately polar compounds, such as those used in this study, the 3-cyanopropylpolysiloxane bonded phases have been found to behave chromatographically like a deactivated silica gel column [22,23]. Residual surface silanols were believed to substantially control the retention under those conditions. From the present data and our prior experience with supercritical CO_2 as an eluent, we speculate that the addition of liquid CO_2 to the mobile phase initially lowers the asymmetry of the chromatographic band because it is more polar than *n*-hexane. However, when more than 0.50 mole fraction of CO_2 is added to hexane, the stationary phase may begin to expand slightly (as is often the case with supercritical CO_2) and then more surface silanols are exposed on the support which causes the increased band broadening with mixture compositions of 0.7 and 1.0 mole fractions of CO_2.

Because of the mixed retention mode (combined interaction of silanols and cyano groups with solutes) of the cyano phase, amines are often added to the mobile phase for complexing with the surface silanol groups. Additional studies to develop and further understand enhanced-fluidity normal-phase separations are presently underway. The addition of a more polar modifier to the eluent should provide better capping of the surface silanols; then the expected increase in efficiency should be more readily apparent when CO_2 is added to the mixture.

4. Conclusions

In previous published work on reversed-phase separations we illustrated that by using enhanced-fluidity liquid mixtures as eluents the pressure

drop across a chromatographic column was diminished, as well as that the efficiency and speed of separation increased. This study was an initial step to analyze the attributes of enhanced-fluidity liquid mixtures for normal-phase chromatography. The viscosity of the eluent was lowered by adding CO_2 to *n*-hexane which resulted in substantially decreased pressure drop across the chromatographic column and increased solute diffusion in the eluent. The linear velocity range and the length of the chromatographic column in HPLC is often limited by the viscosity of the mobile phases employed and the unreasonable head pressures needed to achieve fast linear velocities. The low viscosities and pressure drops attained by using enhanced-fluidity mixtures as mobile phase for HPLC will extend the operable linear velocity range and/or the length of the chromatographic column in HPLC. Extending the linear velocity range will lead to faster separations, while the use of longer columns will provide more total theoretical plates for resolution of complex samples.

However, gains in efficiency were only observed for specific mixtures of hexane–CO_2. This trend correlates closely with the observed trend in peak asymmetry, where enhanced-fluidity mixtures of 0.33 and 0.50 mole fractions of CO_2 in *n*-hexane provided chromatograms with the most symmetric peaks. Variations in solute interactions in the bulk mobile phase or the stationary phase when CO_2 was added, probably caused changes in peak asymmetry and also controlled the measured efficiency. Resistance to mass transfer in the bulk mobile phase or in the stagnant mobile phase of the pores was not the controlling force that caused the chromatographic band shape for some of the hexane–CO_2 mixtures. More studies are necessary to determine whether small proportions of polar cosolvent can stop the variation of peak asymmetry with added CO_2. Only then will the lowered solvent viscosity have a measurable effect on the chromatographic efficiency. These experiments are presently underway.

Acknowledgements

We thank Qin Chen for measuring the polarity of the mixtures. We gratefully acknowledge the support for this work by the National Science Foundation under Grant CHE-9118913.

References

[1] Y. Cui, Ph.D. Dissertation, The Ohio State University, Columbus, OH, 1992.
[2] S.T. Lee and S.V. Olesik, Anal. Chem., 66 (1994) 4498.
[3] Y. Cui and S.V. Olesik, J. Chromatogr. A, 691 (1994) 151.
[4] Y. Cui and S. Olesik, Anal. Chem., 63 (1991) 1812.
[5] A.W. Francis, J. Am. Chem. Soc., 58 (1954) 1099.
[6] K. Ohgagaki and T. Katayama, J. Chem. Eng. Data, 21 (1976) 53.
[7] J.P. Foley and J.G. Dorsey, Anal. Chem., 55 (1983) 730.
[8] J.J. Kirkland, W.W. Yau, H.J. Stoklosa and C.H. Dilks Jr., J. Chromatogr. Sci., 15 (1977) 303.
[9] B.A. Bidlingmeyer and F.V. Warren Jr., Anal. Chem., 56 (1984) 1583A.
[10] A. Berthod, J. Liq. Chromatogr., 12 (1989) 1187.
[11] P.C. Sadek, P.W. Carr, R.M. Doherty, M.J. Kamlet, R.W. Taft and M.H. Abraham, Anal. Chem., 57 (1985) 2971.
[12] M.J. Kamlet, J.L. Abboud and J.L. Taft, J. Am. Chem. Soc., 99 (1977) 6027.
[13] A.S. Teja and P. Rice, in R.C. Reid, J.M. Prausnitz and B.E. Poling (Editors), The Properties of Gases and Liquids, 4th ed., McGraw-Hill, New York, NY, 1987, Ch. 9.
L. Grunberg and A.H. Nissan, in R.C. Reid, J.M. Prausnitz and B.E. Poling (Editors), The Properties of Gases and Liquids, 4th ed., McGraw-Hill, New York, NY, 1987, Ch. 11.
[14] W. Hayduk and S.C. Cheng, Chem. Eng. Sci., 26 (1971) 635.
[15] S.H. Chen, H.T. Davis and D.F. Evans, J. Chem. Phys., 77 (1982) 2540.
[16] A. Bondi, J. Phys. Chem., 68 (1964) 441.
[17] A.L. Meyers and J.M. Prausnitz, Ind. Eng. Chem. Fund., 4 (1965) 209.
[18] J.H. Hildebrand and R.L. Scott, Regular Solutions, Prentice-Hall, New York, NY, 1962.
[19] C. Horváth and H.-J. Lin, J. Chromatogr., 149 (1978) 43.
[20] J.J. Kirkland, J. Chromatogr. Sci., 9 (1971) 206.
[21] L.R. Snyder and J.J. Kirkland, Introduction to Modern Liquid Chromatography, 2nd ed., John Wiley, New York, NY, 1979, p. 791.
[22] P.L. Smith and W.T. Cooper, J. Chromatogr., 410 (1987) 249.
[23] E.L. Weiser, A.W. Salotto, S.M. Flach and L.R. Snyder, J. Chromatogr., 303 (1984) 1.